

# Influence of periapical lesion volume on the radiodensity of surrounding bone: A CBCT study

Matthew Boubaris, Andrew B Cameron, Robert Love, Roy George

School of Medicine and Dentistry, Griffith University, Gold Coast, Australia

## Abstract

**Aim:** This study assesses if the size of periapical lesions has an effect on the bone immediately peripheral to an apical lesion.

**Methods:** Cone-beam computed tomography (CBCT) images of 271 periapical lesions were analyzed using Mimics Research™ to determine the CBCT periapical lesion volume index (CBCTPAVI) score, along with the radiodensity of the lesion, lesion border, and surrounding bone in 0.5 mm increments up to 2.0 mm peripheral to the apical lesion. The one-way analysis of variance was used to assess for significant differences in the radiodensity of the lesion, border, and peripheral bone, as well as differences among CBCTPAVI scores.

**Results:** The radiodensity of bone peripheral to the apical lesion increased significantly up to 1.0 mm around the lesion's perimeter. In addition, lesions with higher CBCTPAVI scores showed a significantly greater difference in the radiodensity from the lesion to the lesion border and the peripheral bone, compared to lesions with smaller CBCTPAVI scores.

**Conclusions:** This study for the first time shows the influence of periapical lesion size on the radiodensity of bone peripheral to an apical lesion. Variations in radiodensity at the perimeter of a periapical lesion can be influenced by the size of the lesion, possibly indicating differences in defense response. Knowledge of these phenomena may provide information on bone healing and enhance our understanding of bone peripheral to a periapical lesion.

**Keywords:** Cone-beam computed tomography; endodontics; periapical lesion; radiodensity; volume

## INTRODUCTION

Radiographic images permit the visualization and assessment of the teeth and their supporting apparatus, the periodontal ligament, and surrounding bone.<sup>[1]</sup> This imaging further allows for the evaluation of the radiodensity of these structures.<sup>[2]</sup> Radiodensity varies based on the density of the tissue being assessed and is measured in Hounsfield units (HUs), which represent the degree of X-ray attenuation.<sup>[3]</sup> The denser the tissue, the more the X-rays are attenuated, the more radiopaque the object appears radiographically, and the larger the HU value associated

with the tissue, whereas less dense tissues appear more radiolucent and have a lower HU value.<sup>[4]</sup>

Radiographic radiodensity assessment of bone allows evaluation of the degree of bone mineralization.<sup>[5]</sup> This has multiple applications in dentistry, including in the fields of endodontics and implantology. Evaluating the bone density of the implant site is an important step in implant treatment planning as it has implications on surgical, healing, and prognostic aspects related to the treatment; hence, this is why a categorization system known as Misch bone density classification is used.<sup>[6,7]</sup> In endodontics, bone healing following root canal therapy is monitored over months and years using follow-up radiographs, with cone-beam computed tomography (CBCT) providing rich information.<sup>[2,8,9]</sup> Healing is perceived if there is an increase in the radiodensity of a radiolucent lesion.<sup>[10]</sup> Evaluating

### Address for correspondence:

Prof. Roy George,  
School of Medicine and Dentistry, Griffith University,  
Gold Coast, Australia.  
E-mail: drroygeorge@gmail.com

Date of submission : 04.04.2024


Review completed : 12.04.2024

Date of acceptance : 02.05.2024

Published : 06.06.2024

This is an open access journal, and articles are distributed under the terms of the Creative Commons Attribution-NonCommercial-ShareAlike 4.0 License, which allows others to remix, tweak, and build upon the work non-commercially, as long as appropriate credit is given and the new creations are licensed under the identical terms.

**For reprints contact:** WKHLRPMedknow\_reprints@wolterskluwer.com

Access this article online	
<b>Quick Response Code:</b> 	<b>Website:</b> <a href="https://journals.lww.com/jcde">https://journals.lww.com/jcde</a>
	<b>DOI:</b> 10.4103/JCDE.JCDE_178_24

**How to cite this article:** Boubaris M, Cameron AB, Love R, George R. Influence of periapical lesion volume on the radiodensity of surrounding bone: A CBCT study. J Conserv Dent Endod 2024;27:626-33.

the changes in radiographic radiodensity is important in assessing changes in bone mineralization in the periapical area, and thus, may provide valuable prognostic information on the healing of periapical lesions.<sup>[2]</sup> Alagl *et al.*<sup>[10]</sup> indicated that an increase in bone radiodensity in the region of the periapical lesion may be useful in detecting bone growth and thus healing.

CBCT provides a more accurate method of assessing periapical changes compared with the two-dimensional radiograph, as it permits assessment of the true, three-dimensional (3D), size of the lesion by means of volume measurement.<sup>[11,12]</sup> Volume of periapical lesions can be classified using the CBCT periapical volume index (CBCTPAVI).<sup>[13,14]</sup> Periapical lesion volume has been correlated with endotoxin levels and healing outcomes post endo-microsurgery.<sup>[11]</sup> In addition, changes in periapical lesion volume have been used to evaluate postoperative healing.<sup>[15]</sup> Thus, assessment of volume and bone density could provide information on the status of bone and allow for assessment of healing in three dimensions, enhancing treatment planning and the assessment of prognosis and endodontic therapy success.<sup>[2,10]</sup> Importantly, investigating the effect of lesion size on the surrounding periapical bone may allow for assessment of the body's response to different-sized lesions, possibly allowing for assessment of the lesion's activity. With the uptake of artificial intelligence (AI) in the assessment of radiographs,<sup>[16]</sup> these data could possibly aid the clinician in the diagnosis and development of techniques to ensure better management of bone during periapical surgery.

Currently, there are no studies that have assessed the quality of bone around the margins of a periapical lesion. Therefore, the aim of this study was to assess the radiodensity of periapical lesions, the lesion border, and peripheral bone within a cone-beam image and its relation to the CBCTPAVI.

## METHODS

Ethical clearance for this study was obtained from the Griffith University Human Research Ethics Committee (EC00162). For the purpose of testing the aim of the study, 271 periapical lesions, along with the border and surrounding bone, were three dimensionally segmented and assessed for variations in bone radiodensity.

### Cone-beam computed tomography selection

CBCT images included in this study were obtained from the Griffith University CBCT archive. For standardization, all images included were acquired using the same CBCT scanner (Carestream CS 9600 CBCT Scanner, Carestream Dental LLC, Georgia, USA), with the following parameters. Teeth with periapical radiolucency were included in the

study; however, cases where two or more adjacent teeth had periapical lesions that coalesced were excluded. The tooth number, as well as the patient's age and gender, was recorded.

### Lesion volume and CBCTPAVI score

3D medical imaging analysis software, Mimics Research™ (v21.0.0.406, Materialise NV, Leuven, Belgium), was used to determine the lesion volume and CBCTPAVI score, following Boubaris *et al.*'s<sup>[14]</sup> methodology. The semi-automatic segmentation technique was used to segment out each periapical lesion from the CBCT data using a mask, which is an adjustable highlighted area on the image slices [Figure 1a]. The segmented mask was converted into a standard tessellation language (STL) file of the lesion to allow visualization in three dimensions. The volume of the lesion was then recorded and a corresponding CBCTPAVI score was assigned to each lesion [Table 1].

### Radiodensity

Mimics™ (Materialise, Leuven, Belgium) was then used to determine the radiodensity of the lesion, lesion border, and bone 0.0–0.5 mm, 0.51–1.0 mm, 1.01–1.5 mm, and 1.51–2.0 mm peripheral to the apical lesion. Rescaling of the lesion, mask subtraction process, and radiodensity measurement were the steps developed in this methodology to permit radiodensity assessment.

### Rescaling the initial lesion

Rescaling indicates that the STL of the lesion was either expanded (to include surrounding structures) or contracted (to remove internal structures) at specified distances around the perimeter of the lesion. The initial STL of each lesion was expanded uniformly by 0.5 mm, 1.0 mm, 1.5 mm, or 2.0 mm using the rescale 3D object tool [Figure 2, step 1] to create STLs of the lesions that included a 0.5 mm, 1.0 mm, 1.5 mm, or 2.0 mm perimeter. In addition, the STLs of the lesions were contracted uniformly by 0.1 mm to create an STL of the lesion without a 0.1 mm border. A mask of each rescaled STL was then created using the “create mask from 3D object” tool [Figure 2, step 2].

### Mask subtraction process

Using the initial lesion masks and the newly created masks, mask subtraction was performed whereby one mask was subtracted from another to create a new resultant mask. This was done using the subtractive “Boolean operations” tool [Figure 2, step 3]. This then allowed the border of the lesion as well as the areas 0.0–0.5, 0.51–1.0, 1.01–1.5, and 1.51–2.0 mm peripheral to the lesion to be analyzed as separate masks.

### Radiodensity measurements

The masks of the area surrounding the lesion were evaluated by two calibrated assessors, and irrelevant

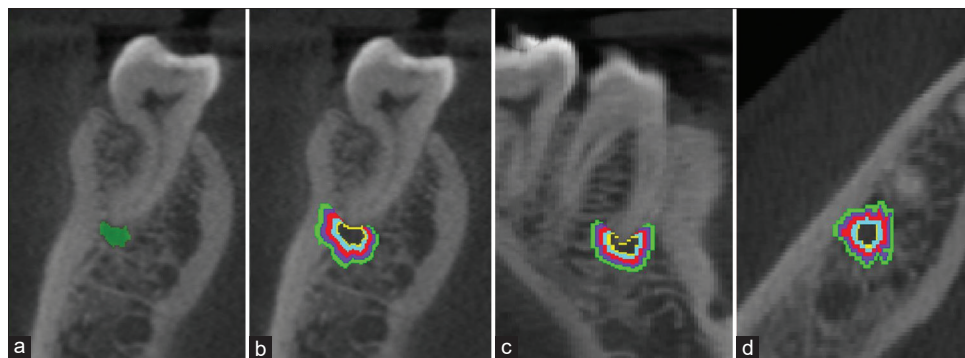


**Figure 1:** (a) Mask of the segmented periapical lesion in the coronal slice. Masks of lesion border (yellow), bone 0.0–0.5 mm (blue), 0.51–1.0 mm (red), 1.01–1.5 mm (purple), and 1.51–2.0 mm (green) peripheral to the lesion for radiodensity measurements in (b) coronal, (c) sagittal, and (d) axial slices

**Table 1: Cone-beam computed tomography periapical lesion volume index scores<sup>[14]</sup>**

CBCTPAVI score	Volume, V (mm <sup>3</sup> )
0	0
1	0.01–0.20
2	0.21–0.70
3	0.71–8.00
4	8.01–70.00
5	70.01–100.00
6	100.01+

CBCTPAVI: Cone-beam computed tomography periapical lesion volume index

structures, including the maxillary sinus, inferior alveolar nerve, adjacent teeth, or air spaces, were removed manually to ensure that only bone was included in the mask [Figures 1b-d and 2 step 4]. The radiodensities of the initial lesion, lesion border, and bone 0.0–0.5 mm, 0.51–1.0 mm, 1.01–1.5 mm, and 1.51–2.0 mm peripheral to the apical lesion were then recorded in HUs utilizing the automated features in the software.

### Change in radiodensity

The radiodensity measurements recorded in the previous step were then used to determine the change in radiodensity from the lesion to the border and the bone peripheral to the lesion. This was done in Microsoft® Excel® (Microsoft®, Washington, USA) by subtracting the radiodensity measurement of the lesion from the radiodensity measurement of the border or bone peripheral to the lesion to determine the change in radiodensity between the two locations.

### Analysis of results

Data analysis was conducted using SPSS Statistics (v26.0.0.1, IBM, New York, USA). The data for radiodensity and change in radiodensity were assessed for normality using the Kolmogorov–Smirnov test. The one-way analysis of variance (ANOVA) was used to assess for differences in the radiodensities of periapical lesions compared to the radiodensities of the lesion border and peripheral bone, as well as differences in the change in radiodensity

from the lesion to the lesion border and peripheral bone among CBCTPAVI scores. *Post hoc* testing was conducted using the Tukey test where equal variance was observed, and the Games–Howell test where equal variance was not observed. The level of significance used for the inferential statistics conducted was  $P < 0.05$ .

### Misch bone density classification

To relate these radiodensity values to a clinically relevant scale for the purpose of communication, assessment, and treatment delivery, the average radiodensity of the periapical lesion, lesion border, and peripheral bone was categorized according to the Misch bone density classification: D1, dense cortical bone (>1250 HUs); D2, dense-to-thick, porous cortical and coarse trabecular bone (850–1250 HUs); D3, thin, porous cortical and fine trabecular bone (350–850 HUs); D4, fine trabecular bone (150–350 HUs); and D5, immature, nonmineralized bone (<150 HUs).<sup>[6,7]</sup>

## RESULTS

The lesions included in this study were associated with the following teeth: sixty (22.14%) mandibular molars, 91 (33.58%) maxillary molars, 15 (5.54%) mandibular premolars, 35 (12.92%) maxillary premolars, 4 (1.48%) mandibular canines, 11 (4.06%) maxillary canines, 16 (5.90%) mandibular incisors, and 39 (14.39%) maxillary incisors. The mean age of the patients included in this study was 56 years (standard deviation [SD], 15), of which 67 (57.26%) were female and 50 (42.74%) were male.

### Radiodensity

The results from the one-way ANOVA test [Table 2] showed that there were significant differences among the radiodensity of the lesion, border, and peripheral bone ( $F = 82.976, P < 0.001$ ). Specifically, it was found that the lesion was significantly less radiodense than the border and the bone 0.0–0.5, 0.51–1.0, 1.01–1.5, and 1.51–2.0 mm peripheral to the lesion. Furthermore, the

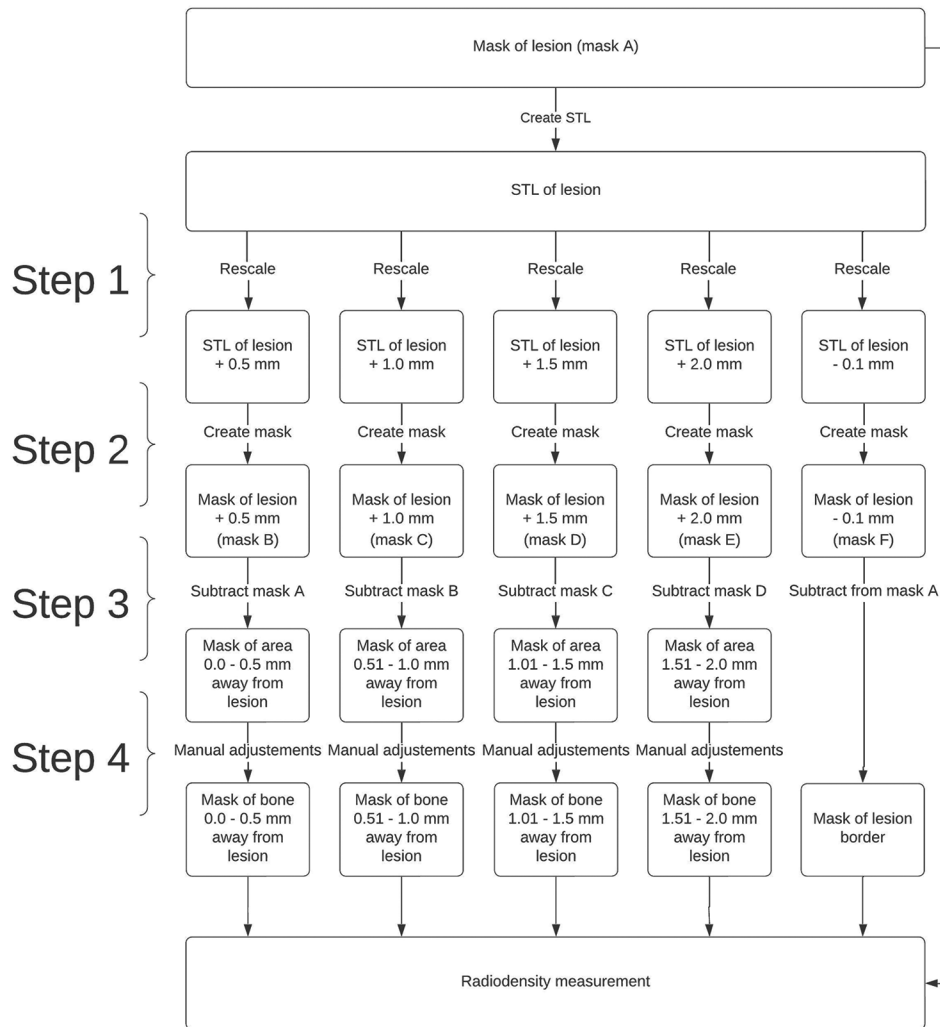


**Figure 2:** Flowchart of methodology showing creation and use of three-dimensional masks of the periapical lesion, lesion border, and surrounding bone to determine radiodensity. The methodology involved the creation of rescaled standard tessellation language (STL) files of the lesions (step 1), the creation of masks from the rescaled STL files (step 2), mask subtraction process (step 3), and manual adjustments to the masks (step 4). STL: Standard tessellation language

border had a significantly lower radiodensity than the bone 0.0–0.5, 0.51–1.0, 1.01–1.5, and 1.51–2.0 mm peripheral to the lesion; and the bone 0.0–0.5 mm peripheral to the lesion was significantly less radiodense than the bone 0.51–1.0, 1.01–1.5, and 1.51–2.0 mm peripheral to the lesion. Moreover, when applying the Misch bone density classification to the results in this study, the average radiodensity of the lesion, lesion border, and bone 0.0–0.5 mm peripheral to the lesion could all be classified as D3 [Table 2]. In addition, the average radiodensity of the bone 0.51–2.0 mm peripheral to the lesion could be classified as D2.

### Change in radiodensity and CBCTPAVI

Significant differences were observed in radiodensity changes among CBCTPAVI categories [Table 3]. The results showed that in all situations where statistical significance was observed, lesions with higher CBCTPAVI scores showed

a significantly greater difference in the radiodensity from the lesion to the lesion border and the peripheral bone, compared to lesions with smaller CBCTPAVI scores. The most notable differences were observed between the lesion and lesion border. Small lesions classified as CBCTPAVI 1 or 2 showed an increase of only 10.39 HU (SD, 12.28 HU) and 28.21 HU (SD, 27.76 HU) from the lesion to the border, respectively, while large lesions classified as CBCTPAVI 5 or 6 showed increases of 187.09 HU (SD, 76.08 HU) and 249.65 HU (SD, 90.48 HU), respectively.

## DISCUSSION

Significant differences were observed between the radiodensity of the lesion, border, and bone peripheral to the apical lesion. When radiodensities of bone peripheral to the lesion were assessed at 0.5 mm increments around the perimeter of the lesion, an increase in radiodensity

**Table 2: Overall mean radiodensity of periapical lesion, periapical lesion border, and peripheral bone**

Variable	Lesion (A) (n=271)	Border (B) (n=271)	0.0-0.5 mm (C) (n=271)	0.51-1.0 mm (D) (n=271)	1.01-1.5 mm (E) (n=271)	1.51-2.0 mm (F) (n=271)	F	Post hoc
Radiodensity (HU), mean (SD)	453.50 (380.72)	598.83 (386.40)	808.15 (404.35)	971.26 (426.15)	983.30 (433.64)	988.36 (433.21)	82.976 (P<0.001)	A<B* A<C, D, E, F** B<C, D, E, F** C<D, E, F**
Misch classification	D3	D3	D3	D2	D2	D2		

\* P<0.01, \*\* P<0.001. 0.0, 0.5, 1.0, 1.5, and 2.0 indicate the bone at specified distances from the lesion perimeter. SD: Standard deviation, HU: Hounsfield unit

was noted only up to 1.0 mm. This could suggest that the inflammatory processes of periapical lesions effect the mineralization of the periapical bone up to 1.0 mm around the perimeter of a lesion. There is a demineralization of the bone in this area before the bone radiodensity and mineralization return to its normal, unaffected, level at 1.0 mm away from the lesion.

The CBCTPAVI, first introduced by Boubaris *et al.*,<sup>[14]</sup> allows for an accurate representation of the 3D size of periapical lesions. When assessing the relationship of CBCTPAVI scores to the change in radiodensity from the periapical lesion to the lesion border and peripheral bone, greater increases in radiodensity were observed with lesions of higher CBCTPAVI scores than with lesions of smaller CBCTPAVI scores. The greatest differences were observed between the lesion and lesion border. For example, lesions classified as CBCTPAVI 6 showed a 24 times greater increase in radiodensity than those classified as CBCTPAVI 1, and a 9-fold increase compared to lesions classified as CBCTPAVI 2. In addition, lesions classified as CBCTPAVI 5 showed an 18 times greater increase in radiodensity than those classified as CBCTPAVI 1, and a 7-fold increase compared to lesions classified as CBCTPAVI 2. All differences observed among CBCTPAVI scores in the radiodensity change between the lesion and peripheral bone were only up to a maximum of 3-fold differences. The greater increase in mineralization associated with larger lesions may indicate the body's increased preparedness for and resistance to larger infections, as the body may have increased time to pick up defenses against larger lesions. Czelej-Górski *et al.*<sup>[17]</sup> observed similar increased defenses by the body to chronic lesions when investigating root densities. They indicated that the root density of teeth associated with chronic periapical changes was increased compared with the root density of healthy teeth or those associated with acute apical inflammation. In addition, the greater increase in radiodensity from larger lesions may also indicate that larger lesions have reduced radiodensity and thus greater demineralization in comparison to smaller lesions. This might be explained by the work of Cardoso *et al.*<sup>[11]</sup> who indicated that lesions of larger volume had increased levels of endotoxins and bacterial counts. As endotoxins and bacteria are responsible for initiating osteoclastic bone resorption, larger lesions that have increased levels of endotoxins and bacterial counts may have reduced bone mineralization due to increased resorption.<sup>[18,19]</sup>

The bone demineralization that occurs in the periapical area is due to an immune response in that region triggered by bacteria.<sup>[19]</sup> Osteoclastic bone resorption is initiated by numerous factors, including bacterial lipopolysaccharides, prostaglandins, and pro-inflammatory cytokines.<sup>[18-20]</sup> The demineralization effect that the periapical lesion has on the peripheral bone, observed in this study, likely indicates osteoclastic activity in the bone adjacent to the lesion due

**Table 3: Mean differences in radiodensity: Periapical lesion versus lesion border and peripheral bone**

Mean differences in radiodensity (HU)	Mean (SD)						F	Post hoc
	CBCTPAVI 1 (A) (n=7)	CBCTPAVI 2 (B) (n=28)	CBCTPAVI 3 (C) (n=71)	CBCTPAVI 4 (D) (n=109)	CBCTPAVI 5 (E) (n=19)	CBCTPAVI 6 (F) (n=37)		
Border versus lesion	10.39 (12.28)	28.21 (27.76)	94.12 (61.05)	174.74 (88.73)	187.09 (76.08)	249.65 (90.48)	42.479 (P<0.001)	A<C, D, E, F*** B<C, D, E, F*** C<D, E, F*** D<F***
0.0–0.5 mm versus lesion	209.74 (119.26)	239.69 (110.39)	310.83 (134.06)	378.93 (132.26)	374.53 (143.40)	471.41 (149.73)	13.752 (P<0.001)	A<D* A<F*** B<D, F*** B<E* C<D* C<F*** D<F**
0.51–1.0 mm versus lesion	363.66 (150.95)	327.72 (154.76)	424.02 (195.75)	558.87 (184.91)	568.89 (215.12)	723.27 (223.84)	19.468 (P<0.001)	A<F*** B<D, E, F*** C<D, F*** C<E* D<F***
1.01–1.5 mm versus lesion	395.42 (262.98)	286.69 (174.74)	411.85 (242.40)	579.66 (203.25)	617.42 (230.91)	773.65 (286.12)	20.805 (P<0.001)	A<F*** B<D, E, F*** C<D, F*** C<E** D<F***
1.51–2.0 mm versus lesion	366.84 (311.09)	279.47 (199.95)	391.07 (279.33)	588.22 (212.28)	627.75 (232.74)	830.91 (268.28)	24.563 (P<0.001)	A<F*** B<D, E, F*** C<D, F*** C<E** D<F*** E<F*

\* P<0.05, \*\* P<0.01, \*\*\* P<0.001. 0.0, 0.5, 1.0, 1.5, and 2.0 mm indicate the bone at specified distances from the lesion perimeter. SD: Standard deviation, HU: Hounsfield unit, CBCTPAVI: Cone-beam computed tomography periapical lesion volume index

to inflammatory mediators in the area. Immunological studies could assess the cells and mediators present at the interface between the periapical lesion and the peripheral bone as analysis of the cells and mediators present in such areas may provide useful information on the processes responsible for the demineralization of the peripheral bone.<sup>[20]</sup>

Peri-radicular curettage is a surgical procedure to remove diseased or reactive tissue from the alveolar bone in the peri-radicular or lateral region surrounding a pulpless tooth.<sup>[21]</sup> While there is evidence that the inflamed soft tissue in the peri-radicular region does not have to be entirely removed,<sup>[22]</sup> there is no evidence of the consequences of leaving remnants of cystic epithelium behind, and because of the inability of a clinician to histologically distinguish tissue, there is a general tendency to ensure that all tissue is removed. This process could lead to unwanted removal of alveolar bone. From a clinical point of view, the use of novel technology (e.g. Piezotronics), that comes with presets to remove specific densities of tissue, may assist in managing tissues more efficiently and carefully at the lesion boundaries during apical surgery, thus enhancing endodontic microsurgery and limiting damage to bone.<sup>[23]</sup> While the Misch bone density classification provides a method to classify bone into five categories (D1–D5) according to bone quality and radiodensity in HUs,<sup>[6,7]</sup> the current classification, with its large HU variations, does not allow differentiation between the lesion, border, and bone 0.0–0.5 mm peripheral to the apical lesion, as it classifies all three regions as D3. Misch classification could be modified to better define the quality of bone in the periapical area when using CBCT and this may be useful in the assessment of healing, communication between clinicians and radiologists, and in developing piezoelectric systems with presets for apical surgeries. Further studies, however, would be needed to identify ideal HU boundaries to modify the Misch classification for the radiographic assessment of periapical healing.

Previous studies have made attempts to investigate periapical lesion radiodensity in HUs, pre- and post-treatment, to assess healing using CBCT. Kaya *et al.*<sup>[2]</sup> examined periapical lesions in the anterior maxilla and Alagl *et al.*<sup>[10]</sup> analyzed periapical lesions in immature teeth. Both studies found that the radiodensity of 80%–100% of periapical lesions could be classified as D5 before treatment and that the radiodensity of 88%–90% of periapical lesions could be classified as D3 1–2 years posttreatment. There are numerous methodological differences between the present study and those conducted by Kaya *et al.*<sup>[2]</sup> and Alagl *et al.*<sup>[10]</sup> that make it difficult to draw comparisons between the results. First, the present study considers the average radiodensity of the entire periapical lesion, while the previous studies have considered the radiodensity from a 2.25 or 3.5 mm<sup>2</sup> region of interest where bone density

was lowest. This may account for the large percentage of D5 radiodensity areas observed pretreatment. In addition, the previous studies only considered large periapical lesions, 8–10 mm in diameter or 4–8 mm in diameter, respectively, versus the present study which only excluded cases where two or more adjacent teeth had periapical lesions that were joined. In addition, the previous studies had small sample sizes of 16 and 10 periapical lesions, respectively, compared with the much larger sample size of 271 in the present study. Furthermore, the previous studies differentiated the radiodensity of periapical lesions pre- and posttreatment, compared to the present study where the samples used represented a mixture of treated and untreated lesions. While this is a limitation of the present study, the results still provide valuable information on the effect of periapical lesions on the surrounding bone.

Several authors have reported that HU measurements obtained from different CBCT scans may show variations.<sup>[24,25]</sup> However, the radiodensity measurements for each sample in this study were taken from the same CBCT scan and were used primarily as a method of comparing the tissue densities within the same image, to evaluate the effect of periapical lesions on the surrounding bone. In addition, all scans used in this study were acquired with the same CBCT machine and exposure factors.

Further studies correlating the current data with histological and immunological data will provide further information regarding the biological processes occurring around lesions of different sizes and may help in validating the results observed in this study. This would contribute to the knowledge obtained from this study regarding the characteristics of periapical lesions and the demineralization effect they have on the peripheral bone up to 1.0 mm away from the lesion. This knowledge may also be useful in developing methods to ensure better management of bone when undertaking periapical curettage. It may also allow for further assessment of lesion activity and healing properties associated with different-sized lesions. From a radiographic reporting point, these data points (volume and radiodensity) could be captured with the development of AI, for example, Diagnocat™ (Diagnocat Inc., San Francisco, CA, USA). The use of AI would drastically reduce the segmentation time and allow clinicians to have a better understanding of the lesion that they may be treating and the characteristics of the surrounding periapical bone.

This study showed for the first time the existence of variations in the bone radiodensity around the perimeter of an apical lesion. This understanding is important as aggressive curettage of the lesion during surgery could not only remove partially demineralized bone but also healthy tissue. In addition, it was observed that lesions of higher CBCTPAVI scores were associated with greater increases in radiodensity around the lesion, possibly indicating an increased defense

mechanism associated with larger lesions. Assessment of radiodensity of the periapical lesion and its surroundings also allows for assessing changes in bone mineralization, providing valuable prognostic information for assessing the healing of periapical lesions after endodontic therapy.

### Acknowledgments

The authors acknowledge support from the Advanced Design and Prototyping Technologies (ADaPT) Institute at Griffith University for Materialise software.

### Financial support and sponsorship

Nil.

### Conflicts of interest

There are no conflicts of interest.

## REFERENCES

1. Yusof Z, Nambiar P. Radiographic considerations in endodontics. *Malays Dent J* 2007;28:51-8.
2. Kaya S, Yavuz I, Uysal I, Akkuş Z. Measuring bone density in healing periapical lesions by using cone beam computed tomography: A clinical investigation. *J Endod* 2012;38:28-31.
3. Shapurian T, Damoulis PD, Reiser GM, Griffin TJ, Rand WM. Quantitative evaluation of bone density using the Hounsfield index. *Int J Oral Maxillofac Implants* 2006;21:290-7.
4. Clementino-Luedemann TN, Kunzelmann KH. Mineral concentration of natural human teeth by a commercial micro-CT. *Dent Mater J* 2006;25:113-9.
5. Valiyaparambil JV, Yamany I, Ortiz D, Shafer DM, Pendrys D, Freilich M, *et al.* Bone quality evaluation: Comparison of cone beam computed tomography and subjective surgical assessment. *Int J Oral Maxillofac Implants* 2012;27:1271-7.
6. Misch CE. Bone character: Second vital implant criterion. *Dent Today* 1988;7:39-40.
7. Misch CE. Density of bone: Effect on treatment plans, surgical approach, healing, and progressive bone loading. *Int J Oral Implantol* 1990;6:23-31.
8. Patel S, Wilson R, Dawood A, Foschi F, Mannocci F. The detection of periapical pathosis using digital periapical radiography and cone beam computed tomography – Part 2: A 1-year post-treatment follow-up. *Int Endod J* 2012;45:711-23.
9. Tiwari UO, Chandra R, Tripathi S, Jain J, Jaiswal S, Tiwari RK. Comparative analysis of platelet-rich fibrin, platelet-rich fibrin with hydroxyapatite and platelet-rich fibrin with alendronate in bone regeneration: A cone-beam computed tomography analysis. *J Conserv Dent* 2020;23:348-53.
10. Alagl AS, Bedi S, Hassan K, Al-Aql Z. Impact of cone beam computed tomography on measurement of bone density in periapical lesions following endodontic treatment: A clinical study. *Biomed Res* 2017;28:7669-74.
11. Cardoso FG, Ferreira NS, Martinho FC, Nascimento GG, Manhães LR Jr., Rocco MA, *et al.* Correlation between volume of apical periodontitis determined by cone-beam computed tomography analysis and endotoxin levels found in primary root canal infection. *J Endod* 2015;41:1015-9.
12. Estrela C, Bueno MR, Leles CR, Azevedo B, Azevedo JR. Accuracy of cone beam computed tomography and panoramic and periapical radiography for detection of apical periodontitis. *J Endod* 2008;34:273-9.
13. Boubaris M, Cameron A, Love R, George R. Sphericity of periapical lesion and its relation to the novel CBCT periapical volume index. *J Endod* 2022;48:1395-9.
14. Boubaris M, Chan KL, Zhao W, Cameron A, Sun J, Love R, *et al.* A novel volume-based cone-beam computed tomographic periapical index. *J Endod* 2021;47:1308-13.
15. Zhang MM, Liang YH, Gao XJ, Jiang L, van der Sluis L, Wu MK. Management of apical periodontitis: Healing of post-treatment periapical lesions present 1 year after endodontic treatment. *J Endod* 2015;41:1020-5.
16. Marwaha J. Artificial intelligence in conservative dentistry and endodontics: A game-changer. *J Conserv Dent Endod* 2023;26:514-8.
17. Czelej-Górski J, Rózyło TK, Rózyło-Kalinowska I. The application of digital radiography and radiodensitometry in evaluation of chronic fibrous periapical changes of endodontically untreated teeth. *Ann Univ Mariae Curie Skłodowska Med* 2001;56:111-8.
18. Stashenko P. Role of immune cytokines in the pathogenesis of periapical lesions. *Endod Dent Traumatol* 1990;6:89-96.
19. Takahashi K. Microbiological, pathological, inflammatory, immunological and molecular biological aspects of periradicular disease. *Int Endod J* 1998;31:311-25.
20. Torabinejad M, Eby WC, Naidorf IJ. Inflammatory and immunological aspects of the pathogenesis of human periapical lesions. *J Endod* 1985;11:479-88.
21. American Association of Endodontists. Glossary: Contemporary Terminology for Endodontics. 5<sup>th</sup> ed. Chicago: American Association of Endodontists; 1994.
22. Gutmann JL, Harrison JW. *Surgical Endodontics*. 1<sup>st</sup> ed. Boston: Blackwell Scientific Publishing; 1991.
23. Abella F, de Ribot J, Doria G, Duran-Sindreu F, Roig M. Applications of piezoelectric surgery in endodontic surgery: A literature review. *J Endod* 2014;40:325-32.
24. Nackaerts O, Maes F, Yan H, Couto Souza P, Pauwels R, Jacobs R. Analysis of intensity variability in multislice and cone beam computed tomography. *Clin Oral Implants Res* 2011;22:873-9.
25. Parsa A, Ibrahim N, Hassan B, Motroni A, van der Stelt P, Wismeijer D. Influence of cone beam CT scanning parameters on grey value measurements at an implant site. *Dentomaxillofac Radiol* 2013;42:79884780.